Korean J. of Chem. Eng., **14**(1), 1-7 (1997)

MEASUREMENT OF COAL PARTICLE SIZE AND SHAPE WITH CONCENTRATED COAL-WATER MIXTURES

Dong-Jin Sung† and Suk-Ho Kang

School of Chem. Eng. & Technol., Yeungnam University, Kyongsan 712-749, Korea
(Received 18 March 1996 • accepted 22 November 1996)

Abstract – The behavior of concentrated coal-water mixtures having narrow particle size fractions of coal was investigated. The pulverized coal was fractionated into six distinct particle size ranges, i.e. −70+80, −80+120, −120+140, −140+200, −200+400 and −400 mesh sizes by using a series of sieves. Settling rates were determined as functions of solids concentration for suspensions in water of coal particles to establish the measurement of particle size and shape factor and to assess concentration effect upon the observed hindered settling rates. The settling rates were modelled using the Richardson-Zaki model with the exponent n variable to account for the nonspherical shape of the coal particles. The data was also correlated with the Michaels-Bolger model which explicitly account for the excess water which is dragged down along with the particles undergoing sedimentation. In addition, coal particles and suspensions were characterized by coal analysis, heating value, solid heat capacity and thermal conductivity, densities, maximum packing concentrations and pore size distributions.

Key words: Coal-Water Mixture, Particle Size, Shape, Settling Rate, Characterization

INTRODUCTION

Particle size and shape are primary properties governing fluid-particle behavior, although often quantitative understanding of their precise roles in influencing the behavior of fluid-particle processes remains uncertain or ambiguous. The nature of fluid-particle and particle-particle interactions depends on particle size, shape and the particle surface characteristics. The strength of particle-particle interactions depends upon particle concentration of the particle-fluid system. Determination of meaningful values for particle size and shape is usually quite difficult and equivocal, because of the vast breadth of the particle size spectrum, and the virtually infinite variety of particle shapes which exist.

The properties of particles are important in so many applications that the aggregate body of available techniques for particle size measurement and particle shape determination are derived from many different disciplines. Among these are soil and mineral physics, surface chemistry, chemical engineering, aerosol science, catalysis, geology, hydrology, and pigment, ceramics, clay and powder technology, to mention a few. The measurement methods generally represent suitable adaptations of known scientific principles and techniques appropriate to the particle size involved.

This paper is concerned with the measurement and correlation of the particle size and shape with concentrated coal-water mixtures (CWM). The concentrated CWM are of interest because of their promise as coal-based fuels processing liquid-fuel attributes. Recently, the coal-water fuels (CWF) preparation and utilization processes have received much attention due to the projected future need to be used more coal as an energy source. A lot of wet pulverized fine coal have been produced in coal preparation plant. Before ultimate use, many stages are involved: coal pulverization, preparation of slurry, storage, handling and transport, atomization and/or combustion. Such beneficiation is necessary because impurities, such as ash and, in particular, pyritic sulfur, are typically dessiminated through the coal matrix in the forms of inclusions of varying sizes and shapes. Effective removal of such materials requires reduction of the coal down to particle sizes small enough to liberate these inclusions, and then to separate them from the mixture using one or a number of wet processes; washing and flotation and their variants. Indeed, deep cleaning of coal requires reduction of size to very fine levels. There are, therefore, good reasons for seeking an understanding of the behavior of CWM.

In this study, the behavior of concentrated coal-water mixtures (CWM) made up from narrow particle size fractions of coal obtained by sieving were investigated. Settling rates were determined as functions of solids concentration for suspensions in water of coal particles in order to establish the measurement of particle size and shape factor. In addition, particles and suspensions are characterized by coal analyses, determination of heating value, solid heat capacity and thermal conductivity, determination of densities, maximum packing concentrations and pore size distributions for each particle size range. These measured properties are important because coal-water mixtures are used as a fuel.

PREVIOUS WORK AND BACKGROUND INFORMATION

1. Particle Size Measurement

The size of a particle, in the case of a sphere, is uniquely defined by its diameter. For ellipsoids, cylinders, and other isometric particles, two perhaps three or more dimensions are needed

†To whom all correspondences should be addressed.

to define the particle size. For irregularly shaped particles, however, the number of dimensions needed to describe the particle size becomes overwhelming. Furthermore, these parameters would only apply to a single particle and could not be extended to a collection of particles since particle shape is rarely uniform. In these cases, the particle size is often determined by measuring some size dependent property of the particle and relating it to the diameter of a sphere which would give the same measurement. This is known as the equivalent spherical diameter and several of the more common types are given in Table 1.

For a spherical particle with diameter d_{St} falling in Stokes flow the drag force is given by:

$$F_D = 3\pi d_{St}\mu V_\infty = (\mu/6)\, d_{St}^3 g(\rho_s - \rho) \quad (1)$$

in which the second equality is the expression of the net force between gravity and buoyancy. Eq. (1) gives:

$$d_{St} = [18\mu V_\infty/(\rho_s - \rho)g]^{1/2} \quad (2)$$

By definition Eq. (2) gives the Stokes diameter of the particle, and on rearrangement also the Stokes velocity V_∞. Relationships among some of the various equivalent diameters can be established. For example, for a particle with an equivalent drag diameter d_D and volume diameter d_v, falling in Stokes law region, the equality between drag and net gravitational force is given by:

$$3\pi d_D\, \mu V_\infty = (\pi/6) d_v^3 g(\rho_s - \rho) \quad (3)$$

Combining Eqs. (2) and (3) we get:

$$d_{St} = (d_v^3/d_D)^{1/2} \quad (4)$$

Eq. (4) is useful because the drag diameter is difficult to measure. Experimental measurements by Pettyjohn and Christiansen [1948], using isometric nonspherical particles, yield the following approximate relationship:

$$(d_{St}^2/d_v^2) \approx \sqrt{\Psi} \quad \text{for } \Psi > 0.67 \quad (5)$$

in which the sphericity, Ψ, defined as the ratio of the surface area of a sphere with the same volume as the particle to the surface area of the particle:

$$\Psi = (d_v/d_s)^2 \quad (6)$$

Accordingly, Eqs. (4)-(6) give $d_D \approx d_s$, whose approximation is subject to the limitations governing Eq. (5) for particles with $\Psi > 0.67$, falling in the Stokes flow regime. The approximation in Eq. (5) may be used as a qualitative measure on the departure of the particle from spherical shape for which $\Psi = 1$.

Particle shape effects on settling velocity have been investigated by McNown and Malaika [1950]. They have calculated the settling velocities at low Reynolds number of ellipsoidal particles by evaluating the integrals in the Oberbeck's equation. For nonspherical particles Stokes drag force expression is modified according to the equation:

$$F = (3\pi\mu V_\infty d_v) K \quad (7)$$

The shape factor K is the ratio of the settling velocity of the volume equivalent sphere, $V_{\infty s}$, to the settling velocity of the particle V_∞. Combining Eqs. (1), (4) and (7) the Stokes law shape factor K can be present by:

$$K = \frac{d_D}{d_v} \quad (8)$$

Table 1. Effective particle diameters and particle size averages

	Effective particle diameters	
d_v=vol. dia.	dia. of sphere with same volume as particle	$d_v=(6V/\pi)^{1/3}$
d_s=surface dia.	dia. of sphere with same surface as particle	$d_s=(S/\pi)^{1/2}$
d_{sv}=surface-vol. dia.	dia. of sphere with same external surface to vol. ratio as particle	$d_{sv}=d_v^2/d_s^2$
d_D=drag dia.	dia. of sphere with same resistance to motion as particle in the same fluid	
d_f=free-falling dia.	dia. of sphere with same density and free-falling velocity as particle	
d_{St}=Stokes dia.	free-falling dia. of particles in Stokes law region (Re<0.2)	
	Particle size averages	
$\bar{d}^m=\Sigma n_i d_i^m/\Sigma n_i$		
$\bar{d}$=number-length mean dia.		
$(\bar{d}^2)^{1/2}$=number-surface mean dia.		
$(\bar{d}^3)^{1/3}$=number-volume mean dia.		
$d_{WM}=\bar{d}^4/\bar{d}^3$=weight-moment mean dia.		
n_i=number of particles of dia. d_i		

2. Particle Size Statistics

As with most powder materials, the measured particle diameter is rarely uniform for the sample as a whole. Even when the particles are fractionated according to size by sieving methods there invariably is a distribution of particle sizes. Since it is not always convenient to present all of the numbers needed to describe a distribution of particle sizes, mean diameters are used.

The general averaging formula for $\bar{d}^m$ given in Table 1 provides the number-weighted mean of the m-th moment of the size distribution. To establish the corresponding relationships based on mass weighting, we assume that the mass, w_i, and the number, n_i, of particles having equivalent diameter d_i are related by:

$$w_i = n_i \alpha_v \rho_s d_i^3 \quad (9)$$

where α_v is the particle volume coefficient which, like the particle density ρ_s, is assumed to be the same for all particles in the mix. Accordingly, the mass-mean diameter is the same as the weight-moment mean diameter $(\bar{d}^4/\bar{d}^3)$ given in Table 1. A significant measure of the spread of the distribution or particle dispersion is the standard deviation σ defined by:

$$\sigma_N = \{\Sigma n_i (d_i - \bar{d})^2/\Sigma n_i\}^{1/2} = \{\bar{d^2} - (\bar{d})^2\}^{1/2} \quad (10)$$

$$\sigma_M = \{\Sigma w_i (d_i - \bar{d})^2/\Sigma w_i\}^{1/2} = \{(\bar{d}^5/\bar{d}^3) - (\bar{d}^4/\bar{d}^3)^2\}^{1/2} \quad (11)$$

3. Sedimentation

Sedimentation is an important process with many practical applications in the chemical and mining industries. Coal cleaning processes, wastewater treament and paper pulp thickening are a few examples of where gravitational sedimentation is

used in industry. The settling rate is a function of the particle size, shape, density and concentration along with the density and viscosity of the suspending medium. A brief development of the determination of settling rates of multisizes nonspherical particle settling which is more often encountered in industrial practice is as followings.

Settling rates in multiparticle systems are influenced by particle-particle collisions, hydrodynamic interaction and any physicochemical forces which may reside on the surface of the particle. In batch settling, the rate of descent of the suspension-supernatant interface during constant rate sedimentation is determined, which corresponds to the rate of settling, U_c, of the particles. The descending particles are displaced by an equal volume of liquid that rises with a velocity U_w. For a slurry with volume fraction of solids, ϕ, the equation of continuity requires that:

$$\phi U_c + (1-\phi) U_w = 0 \tag{12}$$

Eq. (12) is used to calculate the slip velocity $U=(U_c - U_w)$, which is the relative velocity between the particle and the water, and is the pertinent settling velocity. Thus, we get:

$$U=(U_c - U_w)=U_c/(1-\phi) \tag{13}$$

which is the actual settling velocity of a suspension.

To correlate the settling rates with volume fraction of solids we use Richardson and Zaki's [1954] hindered-settling correlation, given by

$$U=V_\infty(1-\phi)^n \tag{14}$$

where V_∞ is terminal velocity of the single sphere settling alone in the same fluid and n is given as a function of particle to cylinder diameter ratio, d/D, and particle Reynolds number, $Re_t=(d\rho V_\infty/\mu)$, by:

$$n=4.65+19.5\,(d/D) \qquad Re_t<0.2 \tag{15}$$

$$n=4.36+17.6\,(d/D)\,Re_t^{-0.03} \qquad 0.2<Re_t<1 \tag{16}$$

$$n=4.45\,Re_t^{-0.1} \qquad 1<Re_t<500 \tag{17}$$

$$n=2.39 \qquad 500<Re_t<7000 \tag{18}$$

For Reynolds numbers in the Stokes flow regime and negligible wall effect, Eq. (15) gives n=4.65 for spherical particles, which clearly signifies a very strong concentration effect. Chong et al. [1979] have found n to be about 4.8 for spheres, 5.4 for cubic shapes, and 5.8 for brick-like and angular particles, which suggests that particle interaction effects are compounded as the shape departs from spherical geometry, resulting in further retardation of settling rate.

Eq. (14) incorporates an effective volume fraction, $\kappa\phi$ of particle proposed by Michaels and Bolger [1962] and given by

$$U=V_\infty(1-\kappa\phi)^{4.68} \tag{19}$$

which requires the exponent in the Richardson-Zaki equation to be the same as that for spheres, but specifically takes into account the extra water which is dragged down with the particle by replacing the actual solids volume fraction, ϕ, by an effective volume fraction, $\kappa\phi$. The factor κ is always greater than one; its magnitude is an indication of the particle's shape.

DESCRIPTION OF NEW WORK

1. Test Materials

The coal used in this study was taken from a sample of Illinois No. 5 coal obtained from Ziegler Coal Co. (Illinois, U.S.A.), which was received in pulverized form. The granular coal was fractionated into six distinct particle size ranges, i.e. −70+80, −80+120, −120+140, −140+200, −200+400 and −400 mesh, by using a series of sieves that were stacked and placed on a Ro-Tap sieve shaker. The master batch of sieved coal particles was repeatedly subdivided using a riffle sampler to obtain representative test samples of the coal. For all sample preparations, distilled water was used as the suspending medium. Detailed analysis of the coal including proximate and elemental analyses, determination of heating value, measurement of heat capacity, and determination of effective solid thermal conductivity are listed in Table 2.

2. Material Characterization

The densities of the coal particles and of the coal-water mixtures were determined using calibrated pycnometers with a temperature bath at 25°C. For the measurement of densities of the coal powders, dilute aqueous solutions of Triton X-100 (0.01 % by weight) were used to wet and disperse the particles. The coal powders consist of clusters of particles which may be joined at the crystal faces forming compact aggregates or at corners of edges forming strong agglomerates; thus the need for wetting and dispersing agents. The particle size distributions of each sample were determined using the computerized Elzone Counter (Model: 112 LTSNGD/ADC/SSP). This instrument provides a particle volume equivalent spherical diameter.

The Elzone Counter is based on the so-called electrozone principle [Karuhn and Berg, 1982]. When particles in an elec-

Table 2. Ultimate and proximate analysis on Illinois No. 5 coal

Proximate analysis	As received	Moisture free	Dry and ash free
Moisture, %	3.5	-	-
Volatile matter, %	42.0	41.9	45.2
Fixed carbon, %	49.1	50.9	54.8
H-T ash, %	7.0	7.2	-
Ultimate analysis			
Hydrogen, %	5.37	5.16	5.56
Carbon, %	69.15	71.66	77.24
Nitrogen, %	1.47	1.52	1.64
Oxygen, %	15.04	12.36	13.32
Sulfur, %	2.00	2.07	2.23
H-T ash, %	6.97	7.22	-
Sulfur analysis			
Sulfate sulfur, %	0.160	0.166	0.179
Pyrite sulfur, %	0.73	0.76	0.82
Organic sulfur, %	1.11	1.15	1.24
Total sulfur, %	2.00	2.07	2.23
Calorific value, J $kg^{-1}\times10^{-7}$	2.973	3.081	3.321
Thermal conductivity $Wm^{-1}\,K^{-1}$	0.28	-	-
Heat capacity cal $g^{-1}\,K^{-1}$	0.28	-	-

trolyte pass through an orifice, a change in the resistance across the orifice generates a voltage pulse which is detected by electrodes on both sides of the orifice. The pulses are amplified, sized and counted, and the results are fed into a computer which processes the data to give a printout size distribution. The measured particle sizes were presented in the form of frequency and of cumulative distributions in Figs. 1 and 2, respectively. Calculated mean particle sizes and other statistical attributes of the size distributions are listed in Table 3. It is evident from the closeness in values of the means, and the fairly small value of the standard deviations relative to the associated means, i.e. the coefficients of variation, C.V. that the distribution for the five larger size fraction coal samples are fairly narrow. The distribution for the −400 mesh particle size fraction is broad.

The specific surface areas of the test samples were measured using sorption of nitrogen and carbon dioxide at 78 K and 195 K, respectively, and the BET and Dubinin-Polanyi equations. Adsorption isotherms were determined with Micromeritics Accusorb 2100E using both liquid nitrogen and dry ice-acetone baths. Use of nitrogen adsorption for measuring the surface area of microporous materials such as coal has been questioned as giving inaccurately low values [Anderson et al., 1962] because the low liquid nitrogen temperature leads to restricted mass transfer due to contraction of pores and lower diffusion coefficients for the adsorbate. These result in failure to attain equilibrium. Hence, carbon dioxide adsorption was used for the coal test samples. For adsorption measurements, 30 minutes were allowed for each adsorption point. The results are presented in Table 4 for each size range of coal particles.

The pore size distributions of each coal sample were measured using mercury porosimetry. The mercury porosimetry apparatus used in the experiments was the Micromeritics Pore Sizer 9305. Intrusion is accomplished by immersing the material in mercury and isostatistically increasing the pressure. Pore diameter and volume data are obtained from equilibrium pressures and volumes assuming that all the pores are straight cylinders, using the Washburn equation. The results are summarized in Table 4.

In addition to these measurements, the maximum packing

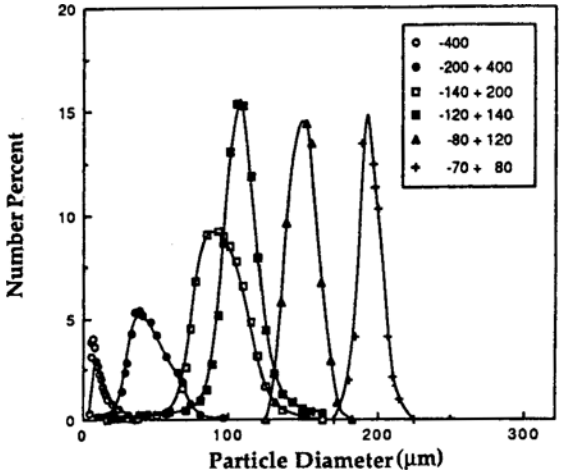

Fig. 1. Particle size distributions for coal particles: frequency plots.

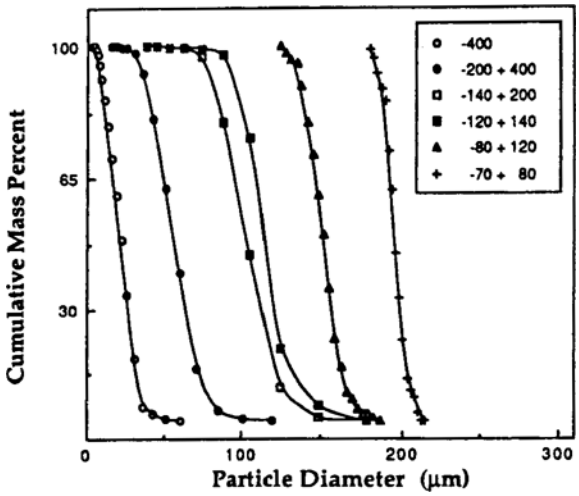

Fig. 2. Particle size distributions for coal particles: cumulative plots.

Table 3. Properties and size analysis of coal particles

Coal	−400	200/400	140/200	120/140	80/120	70/80
ρ_s (g/cm^3)	1.3588	1.3587	1.3580	1.3527	1.3512	1.3478
ϕ_m (v/v)	0.578	0.508	0.520	0.525	0.534	0.556
w_m (w/w)	0.651	0.584	0.595	0.601	0.609	0.629
Mean sieve size (μm)	>38.0	56.5	90.5	115.5	152.5	196.0
Mean particle diameter (μm)						
$\bar{d}$	9.4	41.5	91.4	104.0	150.2	194.7
$(\bar{d^2})^{1/2}$	10.8	44.1	93.4	105.9	150.6	194.9
$(\bar{d^3})^{1/3}$	12.4	46.3	95.0	107.4	151.1	195.0
$(\bar{d^2}/\bar{d})$	12.3	46.8	95.4	107.9	151.0	195.0
$(\bar{d^2}/\bar{d})^{1/2}$	14.2	48.8	96.9	109.2	151.5	195.1
$(\bar{d^3}/\bar{d^2})$	16.3	51.0	98.4	110.5	151.9	195.2
$(\bar{d^4}/\bar{d^3})$	20.6	54.8	101.2	112.6	152.7	195.5
d^b_{N50}	7.8	40.6	92.5	105.3	151.8	193.8
d^c_{M50}	20.3	55.0	100.9	109.9	151.0	194.0
Standard deviation (μm)						
σ_N	5.3	14.8	19.0	20.2	11.0	6.9
C.V. %^{d}	55.9	35.7	20.8	19.4	7.4	3.5
σ_M	8.8	14.2	16.4	15.3	11.6	7.0
C.V. %^{e}	42.8	25.8	16.3	13.6	7.6	3.6

$^b d_{N50}$=number-median diameter
$^c d_{M50}$=mass-median diameter
^{d}C.V.%=$[\sigma_N/\bar{d}]\times 100$
^{e}C.V.%=$[\sigma_M/(\bar{d^4}/\bar{d^3})]\times 100$

Table 4. Surface areas and pore size distributions of test coals

Mesh size	Surface area, m^2/g		Total pore area, m^2/g	Median pore diameter		
	BET	Dub-Pol		Volume	Area	4V/A
−400	218.4	226.9	10.199	2.26	0.013	0.307
200/400	210.2	199.0	0.251	16.31	15.341	14.274
140/200	186.4	132.4	9.542	27.95	0.008	0.337
120/140	165.7	188.9	0.075	35.22	33.763	35.443
80/120	156.4	174.8	17.902	40.45	0.010	0.175
70/80	138.0	160.2	9.898	69.29	0.008	0.291

concentrations for each coal particle size fraction were determined using the irreducible sediment volumes obtained by centrifuging at 7,000 rpm, which is equivalent to 5,019 G force for the rotor used in our centrifuge. A known amount of coal sample was mixed with boiling distilled water for about 10 minutes to obtain uniform wettability between water and coal particles. The slurry was then cooled to room temperature. The sample was then centrifuged for one hour and the excess supernatant was removed. The samples were put back into the centrifuge for another one hour cycle. The sediment was weighed and dried in an oven at 50 °C for 48 hours. The dry sample was weighed and weight fraction was determined by dividing the dry coal weight by the total weight of the sediment. The weight fraction is related to the volume fraction of solid by

$$\text{wt.} = \frac{\rho_s \phi}{\rho_s \phi + \rho_l (1-\phi)} \tag{20}$$

The maximum packing volume fractions of solids obtained from centrifugation experiments are presented in Table 3.

3. Settling Rates of Coal Slurries

The settling velocities of the CWMs were measured using 500 mL graduated cylinders and a constant temperature bath at 25 °C. The CWMs which were previously brought up to experimental temperature in the constant bath were poured into the graduated cylinders until the volume was approximately 500 mL. The cylinders were then covered and were inverted twenty or more times and replaced in the water bath. As the CWM began to settle, the volume of the sediment, V, was recorded as a function of time. Since the cylinders have a constant cross sectional area of 17.02 cm^2, the height of the sediment was easily calculated, h=V/A. The height of the sediment was then plotted against time. The settling velocity of the CWM relative to the container, U_c, was determined by measuring the slope of the linear portion of the height vs. time plot.

Plots of the sediment height as function of time for the 70/80 mesh coal slurries with different initial concentration are given in Fig. 3. The results indicate that constant rate sedimentation is rapidly and unambiguously established for suspensions with this particle size coal and it persists until all particles have settled. The settling rate curves for the slurries made up of the next four smaller test particle size fractions, the 80/120 mesh, 120/140 mesh, 140/200 mesh and the 200/400 mesh coals, were found to be qualitatively identical to those in Fig. 3. There is, however, a marked decrease in the settling rate for the fine coal, −400 mesh coal, given in Fig. 4. Furthermore, the final sediment porosities of the five larger coals are observed to be quite close to the porosities found in the maximum packing configuration whereas there is a significant increase in the porosity for −400 mesh coal. Both of these observations can be explained by the fact that fine particles tend to form loose structures when allowed to settle slowly and that these structures under the stress of their own weight tend to collapse. This in turn squeezes out the excess water which is trapped in the structure causing a decrease in the observed settling rate. When the particles are no longer freely settling the sediment structure continues to collapse as is evidenced by the slow fall of the interface height.

The settling rates for each coal size were correlated with the solids volume fraction using Eqs. (14) and (19). The parameters obtained from fitting the settling data to Eqs. (14) and (19) are given in Table 5. The values of n in Richardson and Zaki's equation, Eq. (14), range from about 5.19 to about 9.04 (for the −400 mesh slurry), which are significantly larger than the accepted value of about 4.68 for hindered settling of spherical particles and indeed larger than the values obtained by Chong et al. [1979] for cubic and angular particles. These results demonstrate that the nonspherical shapes of the coal particle lead to significant further retardation of the settling. The values of

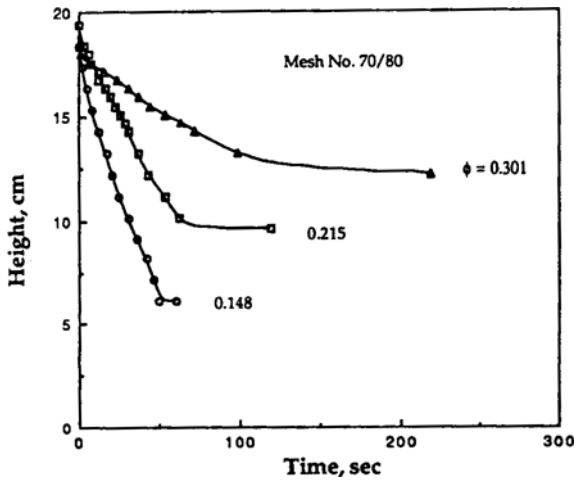

Fig. 3. Settling rate curves for 70/80 mesh coal slurries at 25 °C.

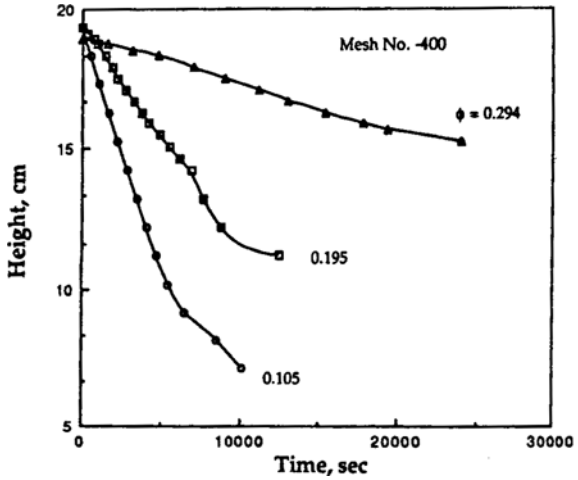

Fig. 4. Settling rate curves for −400 mesh coal slurries at 25 °C.

Table 5. Hindered settling parameters for CWM

Test coal mesh	n	$V_\infty \times 10^3$ cm/s Eq. (14)	d_{St} μm	κ	$V_\infty \times 10^3$ cm/s Eq. (19)	d_{St} μm
−400	9.04	6.1	16.6	1.58	5.1	15.2
200/400	8.66	34.6	39.5	1.82	28.1	35.6
140/200	7.49	181.4	90.6	1.38	163.8	86.1
120/140	5.19	239.6	104.9	1.07	228.4	102.4
80/120	7.67	480.8	148.9	1.40	426.3	140.2
70/80	6.69	821.8	195.6	1.29	800.9	193.1

Table 6. Calculated particle shape factors

Coal sample	− 400	200/400	140/200	120/140	80/120	70/80
d_{St}(μm) Eq. (14)	16.6	39.5	90.6	104.9	148.9	195.6
$d_D \approx \bar{d}^3/d_{St}^2$	3.0	45.8	93.0	102.2	152.8	192.9
$\psi \approx (d_{St}/\bar{d})^4$	9.725	0.821	0.965	1.035	0.966	1.019
$K=(d_D/\bar{d})$	0.319	1.104	1.018	0.983	1.017	0.991
d_{St}(μm) Eq. (19)	15.2	35.6	86.1	102.4	140.2	193.1
$d_D \approx \bar{d}^3/d_{St}^2$	3.6	56.4	102.9	107.3	172.4	197.9
$\psi \approx (d_{St}/\bar{d})^4$	6.837	0.542	0.787	0.940	0.759	0.968
$K=(d_D/\bar{d})$	0.383	1.359	1.126	1.032	1.148	1.016

κ in Table 5 are calculated from settling rate data using Eq. (19) that incoporates an "effective volume fraction" κϕ of particles. These values of κ provide measures of the degree of augmentation of the volume fraction associated with the amount of fluid entrained by the nonspherical, settling coal particle. It is found that for the four larger particle size fractions, this value amounts to approximately 28 %, but it is larger for two smaller particle size fractions for which it is 70 %. This is perhaps due to the additional entrainment of fluid within particle aggregates that are more likely to form which with the smaller particles.

Aside from the foregoing, we used the single-particle Stokes diameters from Table 5 to determine shape parameters for our particles. Since the particle diameter measured using the electric sensing zone principle provides the equivalent spherical diameter, d_v, and the distribution for our five larger particle fractions were fairly narrow it was assumed to be $d_v=\bar{d}$. This permits to estimate the drag diameters from Eq. (4) and the sphericity from Eq. (6), and the shape factor K from Eq. (8). The results are given in Table 6. Since the − 400 mesh size coal fraction is appeared to be too broard for the mean particle diameter $\bar{d}$ to provide a meaningful representation for the equivalent volume diameter d_v the results in Table 6 pertaining to this coal size fraction do not have any significant. However, for the five larger coal size fractions all different equivalent spherical diameters, d_{St}, d_D, and $\bar{d}$ calculated on the basis of the Stokes diameter derived from Richardson and Zaki's correlation are essentially the same, and all shape factors are approximately unity, i.e. Ψ=0.96 and K=1.02. Therefore, the results using this correlation are evidently indifferent to nonsphericity of particle shape. In contrast, the results derived from the correlation involving the effective volume concept, Eq. (19), lead to different conclusions. The particle sphericities for the five larger size fraction coals are found to be about 0.80, while the shape factors K from Eq. (8) are found to be about 1.14. McNown and Malaika [1950] indicated that values of K in the range of $1.10 \leq K \leq 1.15$ define a narrow geometric region in which a variety of particle shapes are subsumed from oblate spheroids through ellipsoids to prolate spheroids. Photomicrographs of our pulverized coals, which provide the projected particle profile indicate that they are plate-like particles with relatively isodimensional, albeit irregularly-contoured, projections. Therefore, we obtain ranges of shape consistent with and subsuming the directly observed shapes of our particles. Quantitative treatment of particle shape to our analysis is seldom attempted in this study.

CONCLUSIONS

The principal conclusions to be drawn from this study are as followings:

1. The settling velocities were correlated in terms of volume fraction using two different methods. (1) the Richardson and Zaki equation with the hindered settling index n (2) the Michaels and Bolger relation which explicitly account for the increase in effective solids volume fraction, κϕ.
2. For the five larger coal size fractions, all different equivalent spherical diameters, d_{St}, d_D and $\bar{d}$ calculated on the basis of the Stokes diameter derived from Richardson and Zaki correlation are essentially the same, and all shape factors are approximately unity, leading to indifference to nonsphericity of particle shape.
3. The particle sphericities for the five larger size fractions obtained from the relation involving the effective volume concept are found to be less than unity as expected for nonspherical particles.
4. Photomicrographical analysis of our pulverized coal particles indicated that they are plate-like particles with relatively isodimensional shape, which is consistent with the range of shape factor K investigated by McNown and Malaika.

NOMENCLATURE

- d : diameter of particle [μm]
- $\bar{d}$: number-mean particle diameter [μm]
- D : cylinder diameter in sedimentation [cm]
- F_D : drag force [N]
- K : ratio of particle drag to volume diameter, Eq. (8)
- n : exponent in Richardson and Zaki model, Eq. (14)
- n_i : number of particles of size x_i, Table 1
- Re_t : particle Reynolds number based on V_∞
- U : sedimentation velocity of suspension [cm/sec]
- U_c : sedimentation velocity of particles relative to container walls [cm/sec]
- U_w : liquid rise velocity relative to particle settling [cm/sec]
- V_∞ : settling velocity of a single particle [cm/sec]
- $V_{\infty s}$: V_∞ for a spherical particle, Eq. (7) [cm/sec]
- w_i : mass of particles with diameter d_i, Eq. (9) [g]

Greek Letters

- α_v : particle-volume shape factor, Eq. (9)
- κ : ratio of effective volume fraction of solids Eq. (19)
- ρ : suspending medium density [g/cm^3]
- ρ_s : suspended solids or particle density [g/cm^3]
- σ : standard deviation, Eqs. (10) and (11)
- ϕ : volume fraction of solids
- ϕ_m : solids volume fraction at maximum packing
- Ψ : sphericity, Eq. (6)

REFERENCES

Anderson, R., Hofer, L. and Bayer, J., "Surface Area of Coal", *Fuel*, **41**, 559 (1962).

Chong, Y. B., Ratkowsky, D. A. and Epstein, N., "Effect of Particle Shape on Hindered Settling in Creeping Flow", *Powder Technol.*, **23**, 55 (1979).

Karuhn, R. F. and Berg, R. H., "Practical Aspects of Electrozone Size Analysis", Particle Data Lab., Elmhurst, IL., 1982.

McNown, J. S. and Malaika, J., "Effects of Particle Shape on Settling Velocity at Low Reynolds Numbers", *Trans. Amer. Geophys. Union*, **31**, 74 (1950).

Michaels, A. S. and Bolger, J. C., "Settling Rates and Sediment Volumes of Flocculated Kaolin Suspensions", *Ind. & Eng. Chem. Fund.*, **1**, 24 (1962).

Pettyjohn, E. S. and Christiansen, E. B., "Effect of Particle Shape on Free Settling Rates of Isometric Particles", *Chem. Eng. Prog.*, **44**, 157 (1948).

Richardson, J. F. and Zaki, W. N., "Sedimentation and Fluidization: I", *Trans. Instn. Chem. Engrs.*, **32**, 35 (1954).